Mineral Petrol (2008) 93: 185–211
DOI 10.1007/s00710-007-0228-y
Printed in The Netherlands

Mineralogy and Petrology

Zircon typologies and internal structures as petrogenetic indicators in contrasting granitoid types from central Anatolia, Turkey

S. Köksal[1], **M. Cemal Göncüoglu**[2], **F. Toksoy-Köksal**[2], **A. Möller**[3,4], **H. Kemnitz**[5]

[1] Radiogenic Isotope Laboratory, Central Laboratory, Middle East Technical University, Ankara, Turkey
[2] Department of Geological Engineering, Middle East Technical University, Ankara, Turkey
[3] Institut für Geowissenschaften, Universität Potsdam, Potsdam-Golm, Germany
[4] Department of Geology, University of Kansas, Lawrence, Kansas, USA
[5] GeoForschungsZentrum Potsdam, Telegrafenberg, Potsdam, Germany

Received December 7 2006; Accepted November 27 2007; Published online February 28 2008

Editorial handling: R. Abart

Summary

The external zircon morphology of granitoid rocks is combined with internal structures studied by cathodoluminescence imaging, to test the classic 'Pupin method' against geological and geochemical evidence for the origin and evolution of granitic rocks.

Granitoids in Central Anatolia display a wide range of petrological characteristics from S-type and I-type to A-type. We studied the morphologies and internal structures of zircons from the Terlemez, Baranadag, Çamsari and the Hisarkaya granitoids from Central Anatolia. The Terlemez and Baranadag quartz-monzonites show a hybridized I-type nature regarding the mineralogy and geochemistry, while the Çamsari quartz-syenite is a typical A-type granitoid. The Hisarkaya porphyritic granite shows fractionated I-type geochemical characteristics, but has significant crustal involvement in its source. In these granitoids, zircon is associated with biotite, quartz, orthoclase, plagioclase, and allanite. Typological investigations after Pupin (1980) along with scanning electron microscope imaging reveal that the external morphology of zircon varies consistently with the granitoid type. Zircon populations of the I-type Terlemez and

Correspondence: S. Köksal, Radiogenic Isotope Laboratory, Central Laboratory, Middle East Technical University, 06531 Ankara, Turkey
e-mail: skoksal@metu.edu.tr

Baranadag quartz-monzonites mainly comprise S-type zircon crystals, with rare J-zircon type, and their typologic evolution trends are consistent with their calc-alkaline hybrid origin. The A-type Çamsari quartz-syenite mainly has K- and V-zircon types and typological evolution trends compatible with those of alkaline granitoids.

The zircons from the Hisarkaya porphyritic granite, on the other hand, show typological characteristics similar to I- to A-type granitoids. However, cathodoluminescence images of zircons from this granitoid imply that the formation of growth zones, including some impurity elements like U, Th, Y, P, and REE at particular magmatic conditions could have resulted in abrupt typological changes during the latest stages of crystallization. The Hisarkaya porphyritic granite is thus an excellent example of the final surface morphologies of zircon not representing the overall general nature of the granitoid.

Cathodoluminescence imaging of internal structures of zircons from the A-type Çamsari quartz-syenite shows extensive metamictization. Moreover, in the zircons from the I-type Terlemez and Baranadag quartz-monzonites, multiple low-luminescent corrosion zones are enriched in U, Th, and Y, and interpreted to result from magma mingling/mixing processes.

Introduction

Zircon, being highly durable to chemical and physical influences, is a particularly useful mineral for petro-chronological investigations. It is one of the most widely used minerals for understanding the petrogenesis of magmatic, metamorphic and sedimentary rocks (e.g., Corfu et al., 2003). Moreover, links between zircon growth and granitoid petrology have been argued for by various studies (e.g., Wang et al., 2002; Belousova et al., 2006; Siebel et al., 2006).

Empirical studies by Pupin (1980) infer that the morphology of zircon reflects the source characteristics of the host-granitoid. Pupin (1980) proposed a scheme relating the external zircon morphology to a genetic classification of the host-granitoid and the temperature of crystallization of the granite magma, and presented the basics of the zircon typology method, in which an arrangement of given prismatic and pyramidal crystal faces constitutes population types. Although *Pupin*'s method has been relevant for various igneous suites, its basics were questioned by several authors (e.g., Vavra, 1990, 1993; Benisek and Finger, 1993) inferring that the morphologies of zircon crystals could only reflect the latest stages of granitoid evolution.

Vavra (1993) indicated that growth rates of zircon crystal faces are controlled by the environmental conditions at any instant, whereas crystal morphology is only the final result from the integration of variable growth rates during previous growth that may have proceeded in a changing crystallization environment. Benisek and Finger (1993) have shown that the size relations of two zircon prism faces are strongly dependent on the chemistry of the growth medium, instead of the temperature of crystallization. All of these views render it necessary to supplement the morphological approach by examination of internal features to obtain reliable data on growth characteristics of zircon within granitoids. Cathodoluminescence (CL) imaging is thus a useful tool for the detection of primary and secondary features preserved in zircon crystals (e.g., Hanchar and Miller, 1993; Hanchar and Rudnick, 1995; Pidgeon et al., 1998).

The petrological characteristics of the Central Anatolian Granitoids (CAG) have been discussed in several studies (e.g., Akiman et al., 1993; Erler and

Göncüoglu, 1996; Boztug, 2000; Düzgören-Aydin et al., 2001; Kadioglu et al., 2003; Ilbeyli et al., 2004; Köksal et al., 2004; Ilbeyli, 2005; Tatar and Boztug, 2005), based mainly on geological and geochemical data. Granitoids from the Terlemez (Terlemez quartz-monzonite), the Baranadag (the Baranadag quartz-monzonite and the Çamsari quartz-syenite), and the Ekecikdag Intrusive Suites (Hisarkaya porphyritic granite) (Central Anatolia) were selected for this study. Zircon, as one of the most common accessory minerals present in the studied granitoids, is found in contact with major phases (biotite, quartz, orthoclase, plagioclase, and allanite) and as inclusions in these minerals. Our study concentrates on zircon crystallization in the chemically distinct granitoid types and how these features may be related. The purpose of this paper is to investigate possible petrological implications of the external morphological and internal structural characteristics of zircon from the selected granitoids. This is the first effort of discussing zircon crystallization features for the petrological characterization of the CAG.

Geological and geodynamic setting

Anatolia is a geologically significant region for the palaeogeographic configuration of continents throughout the opening and closure episodes of the Tethys Ocean.

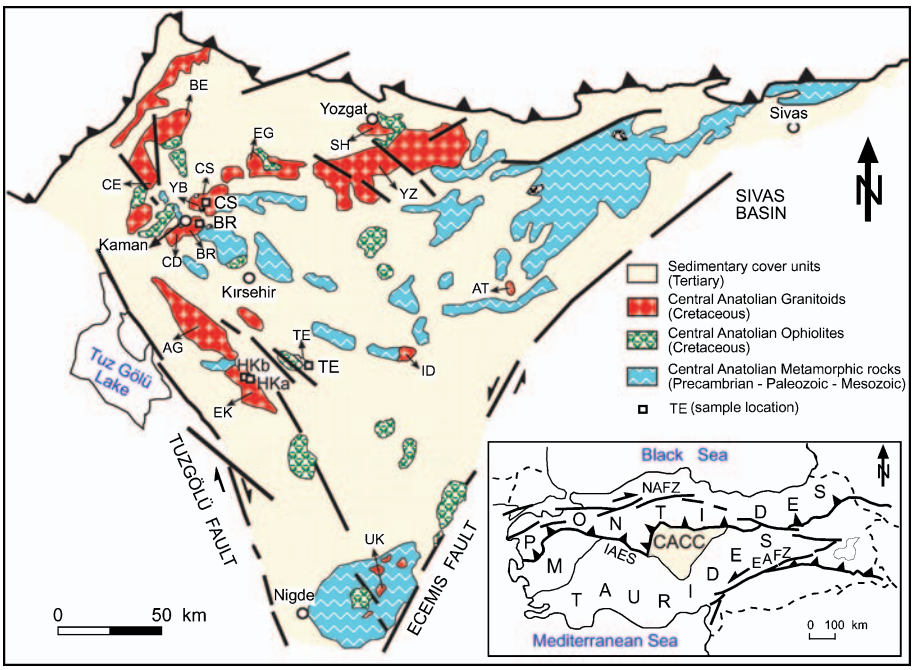

Fig. 1. Simplified geological map of the CACC (Modified after Göncüoglu et al., 1991; Boztug, 2000; Düzgören-Aydin et al., 2001; Toksoy-Köksal et al., 2001) including the sample locations. Inset map shows the main tectonic units in Turkey. Abbreviations: *M* Menderes Massif, *IAES* Izmir-Ankara-Erzincan Suture Zone, *NAFZ* North Anatolian Fault Zone, *EAFZ* East Anatolian Fault Zone. Central Anatolian Granitoids: I-type; *BR* Baranadag, *CD* Cefalikdag, *AG* Agaçören, *TE* Terlemez, *EK* Ekecikdag, *CE* Çelebi, *BE* Behrekdag, *YZ* Yozgat; *HKa* Hisarkaya-a, *HKb* Hisarkaya-b; S-type; *UK* Üçkapili, *SH* Sarihacili; A-type; *CS* Çamsari, *EG* Egrialan, *ID* Idisdag, *AT* Atdere, *YB* Bayindir

The present geology of Anatolia was mainly influenced by the Alpine Orogeny represented by the closure of various branches of the Neo-Tethys Ocean (Sengör and Yilmaz, 1981). Precambrian-Mesozoic metamorphic rocks form the basement of the Central Anatolian Crystalline Complex (CACC) (Fig. 1), and ophiolitic rocks, mainly gabbros, were thrust over this basement (Göncüoglu et al., 1991). The Late Cretaceous granitoids portraying different stages of collisional magmatism intruded the basement rocks and overlying ophiolitic rocks (Göncüoglu et al., 1993; Düzgören-Aydin et al., 2001). Paleocene to Eocene volcanic, volcanoclastic, and carbonate rocks, Oligocene to Miocene evaporites and continental clastic rocks, and Upper Miocene to Pliocene continental clastic, volcanoclastic, and volcanic rocks represent relatively younger units within the CACC (Göncüoglu et al., 1993).

There are different petrogenetic and geodynamic interpretations of the evolution of the CAG. Sengör and Yilmaz (1981) described these granitoids as products of the calc-alkaline magmatism related to the northward-subduction of an ''Inner Tauride Ocean'' beneath the CACC during Lower Paleocene-Eocene. Görür et al. (1984, 1998) on the other hand, relate the granitoids to an Andean-type arc magmatism associated with the eastward subduction of the Inner Tauride Ocean during Paleocene-Early Eocene. Alternatively, Boztug (2000) stated that the crustal metasediments of the CACC could have been affected by inverted metamorphism resulting from the Anatolide-Pontide collision at the northern margin of the Anatolide-Tauride segment that produced the granitoid melts.

Ilbeyli et al. (2004), stating the lack of evidence for localized extension in the CACC, described the mechanism for the initiation of the post-collisional Central Anatolian magmatism to be either thermal perturbation of the metasomatized lithosphere by delamination of the thermal boundary layer, or removal of a subducted plate. In contrast, many other authors (e.g., Göncüoglu et al., 1993, 1997; Göncüoglu and Türeli, 1994; Yaliniz et al., 1999; Aydin et al., 1998; Düzgören-Aydin et al., 2001; Köksal et al., 2001, 2004) describe the granitoids as having evolved through the collision of the northern Tauride-Anatolide platform-margin with a Neo-Tethyan island-arc and subsequent post-collisional extension periods during the Late Cretaceous.

Geological and petrological features

The Central Anatolian Granitoids are commonly subdivided into I-type (i.e., those derived by melting of metaigneous crust; e.g., Chappell et al., 1987), S-type (i.e., those derived from sedimentary protoliths; e.g., Chappell and White, 1974), and A-type (i.e., alkaline, anhydrous and/or anorogenic; e.g., Loiselle and Wones, 1979; Collins et al., 1982; Whalen et al., 1987; or post orogenic, e.g., Bonin et al., 1998). In previous studies (e.g., Otlu and Boztug, 1998; Aydin and Önen, 1999; Yaliniz et al., 1999; Boztug, 2000; Köksal et al., 2004; Ilbeyli et al., 2004; Ilbeyli, 2005) the Terlemez quartz-monzonite from the Terlemez area and the Baranadag quartz-monzonite from the Baranadag area (Fig. 1) were described as I-type CAG. The Baranadag quartz-monzonite is rather evolved and shows transitional features towards A-type, whereas the Çamsari quartz-syenite from the Çamsari area (near Baranadag) was interpreted as an A-type CAG (Fig. 1). The Hisarkaya porphyritic granite (samples Hisarkaya-a and Hisarkaya-b), having features of I-type granit-

oids, has been grouped with the Ekecikdag igneous suite, which comprises S- to I-type granitic rocks (Fig. 1) (e.g., Göncüoglu and Türeli, 1994; Düzgören-Aydin et al., 2001).

The studied granitoids intruded the metamorphic basement and the overlying ophiolitic rocks and are themselves overlain by Late Cretaceous to Paleocene sedimentary rocks. U-Pb titanite ages for the Baranadag quartz-monzonite and Çamsari quartz-syenite date these at 74.0 ± 2.8 Ma and 74.1 ± 0.7 Ma, respectively (Köksal et al., 2004). This is consistent with the result of Ilbeyli et al. (2004), who determined the age of Baranadag quartz-monzonite as 76.4 ± 1.3 by the K/Ar method on hornblende. Based on K–Ar hornblende and K-feldspar isotopic data Yaliniz et al. (1999) interpreted the Terlemez quartz-monzonite to have intruded at 81.5 ± 1.9 Ma and cooled at 67.1 ± 1.3 Ma. However, our unpublished LA-ICP-MS U-Pb zircon data yield 75.0 ± 1.3 Ma age for the Terlemez quartz-monzonite (Köksal et al., unpublished data). For the Hisarkaya porphyritic granite, preliminary results of ongoing LA-ICP-MS U-Pb zircon analyses show an intrusion age of ca. 82 Ma with inherited cores from 143 to 1055 Ma (Köksal et al., unpublished data). These ages demonstrate that the studied granitoids are Late Cretaceous in age. While the monzonitic I-type granitoids and the A-type granitoids cutting and/or co-existing with I-type granitoids have ages around 75 Ma, some 5–9 Ma older S- to I-type intrusions exist in the CACC, like the Hisarkaya porphyritic granite.

The Terlemez and Baranadag quartz-monzonites contain K-feldspar, plagioclase (oligoclase), quartz $\pm$ hornblende $\pm$ biotite $\pm$ clinopyroxene $\pm$ chlorite with accessory zircon, titanite, allanite, and opaque minerals. The Terlemez and Baranadag quartz-monzonites include abundant irregular, angular or sub-rounded mafic microgranular enclaves having sharp contacts to their host (Otlu and Boztug, 1998; Aydin and Önen, 1999; Yaliniz et al., 1999; Köksal et al., 2004). These enclaves are finer grained than their host rock and have been interpreted as evidence for magma mingling processes (Didier and Barbarin, 1991). Moreover, the presence of K-feldspar megacrysts and abundance of mafic minerals (with hornblende > biotite) are characteristic for the Terlemez and Baranadag quartz-monzonites. These features are accepted as the fingerprints of magma mingling/mixing processes (Güleç and Kadioglu, 1998; Kadioglu and Güleç, 1999), and resemble the hybrid-type granitoid series of Barbarin (1990). Therefore, magma mingling/mixing processes between co-existing mantle-derived mafic and crustal-derived felsic magmas are interpreted to have created most of the I-type granitoids in the CACC (e.g., Düzgören-Aydin et al., 2001). Accordingly, Ilbeyli and Pearce (2005) stated that mafic to intermediate enclaves in the I-type CAG indicate interaction between silicic magmas and mantle-derived melts. The Çamsari quartz-syenite on the other hand contains K-feldspar, quartz, plagioclase (An_{21} to An_0) $\pm$ hornblende $\pm$ biotite $\pm$ clinopyroxene, accessory fluorite, titanite, zircon, apatite, and opaque minerals, and has no mafic enclaves (Köksal et al., 2004). The Hisarkaya porphyritic granite consists of K-feldspar, quartz, plagioclase, biotite, hornblende, zircon, apatite and opaque minerals, and minor mafic enclaves with respect to the monzonitic I-type CAG (Göncüoglu and Türeli, 1994; Köksal, 2005), less than 1% CIPW-normative corundum is calculated.

Representative geochemical data from the granitoid samples concerned are given in Table 1. In previous studies (Yaliniz et al., 1999; Köksal et al., 2004;

Table 1. *Geochemical analyses[1] of the studied Central Anatolian Granitoids*

Elements	Samples				
	Baranadag	Terlemez	Hisarkaya-a	Hisarkaya-b	Çamsari
SiO_2	59.6	65.6	71.0	75.1	63.7
Al_2O_3	17.3	15.4	15.0	13.0	18.1
$Fe_2O_3^{tot}$	4.98	4.33	2.06	1.41	2.63
MgO	1.54	1.20	0.51	0.23	0.28
CaO	4.87	4.42	1.95	0.92	1.74
Na_2O	3.49	2.84	3.55	3.10	4.77
K_2O	6.35	4.12	5.09	5.37	7.95
TiO_2	0.53	0.60	0.17	0.10	0.35
P_2O_5	0.24	0.14	0.02	<0.01	<0.01
MnO	0.10	0.08	0.08	0.07	0.06
LOI	0.8	1.1	0.6	0.6	0.6
Total	99.9	100.0	100.2	100.0	100.2
Ba	1114	904	435	290	261
Sc	6	5	3	2	1
Cs	9.3	7.3	6.8	34.3	14.8
Ga	20	25	17	15	22
Hf	7.6	6.8	3.0	3.4	10.3
Nb	24	19	14	19	47
Rb	233	175	266	382	335
Sr	1014	634	119	47	309
Ta	1.3	1.3	1.8	3.3	2.0
Th	27	22	32	35	59
U	6.8	3.6	8.9	10.2	12.5
V	97	53	24	14	40
Zr	275	223	87	73	518
Y	29	21	23	30	24
Cu	19	15	15	9	14
Pb	6.8	9.4	6.0	6.9	29.2
Zn	47	49	33	21	31
Ni	28	25	24	13	22
La	75	52	23	25	148
Ce	151	99	42	43	248
Pr	14.3	9.4	3.9	4.0	18.3
Nd	57.3	37.3	14.5	15.3	58.5
Sm	9.5	6.8	3.1	2.9	7.5
Eu	2.0	1.3	0.5	0.3	1.4
Gd	7.26	5.21	2.54	2.96	6.32
Tb	0.94	0.71	0.53	0.59	0.71
Dy	5.0	3.5	3.4	4	3.9
Ho	0.79	0.68	0.63	0.81	0.66
Er	2.4	2.0	2.3	3.1	2.2
Tm	0.32	0.28	0.34	0.62	0.29
Yb	2.5	2.2	2.6	4.1	2.4
Lu	0.36	0.31	0.45	0.68	0.37
$(Eu/Eu^*)_N$[2]	0.75	0.64	0.52	0.27	0.60
$(La/Yb)_N$[2]	21	16	6	4	42

[1] Geochemical data from granitoids Baranadag and Çamsari are taken from Köksal et al. (2004), Terlemez, Hisarkaya-a and Hisarkaya-b are from this study. Geochemical analyses were performed by ACME Analytical Laboratories Ltd. (Canada). Major elements, Ba, and Sc were measured by ICP-AES

Trace elements excluding Ba and Sc were measured by ICP-MS and LOI is loss on ignition

Tot: total Fe as Fe_2O_3; major elements in wt%; trace elements in ppm

[2] REE data are normalized to Chondrite values of McDonough and Sun (1985)

Köksal, 2005), the Terlemez and Baranadag quartz-monzonites are interpreted as calc-alkaline metaluminous (based on the classifications of Irvine and Baragar (1971) [alkali-silica] and Maniar and Piccoli (1989) [on the basis of Shand's index]), the Hisarkaya porphyritic granite as calc-alkaline and slightly peraluminous, and the Çamsari quartz-syenite as alkaline metaluminous. When classified after Frost et al. (2001), the Terlemez quartz-monzonite shows magnesian calc-alkalic features similar to the most of the Cordilleran granitoids, and the Çamsari quartz-syenite displays ferroan alkalic characteristics as most of the A-type granitoids. The Baranadag quartz-monzonite on the other hand is classified as magnesian alkalic, showing its alkaline affinity based on Frost et al. (2001)'s classification. Furthermore, the Hisarkaya porphyritic granite is classified as magnesian alkali-calcic, yielding similarities to the post-orogenic Cordilleran granitoids based on the same classification scheme, but it should be noted that the peraluminous granitoid might span the whole range of granitoid compositions from magnesian to ferroan, and from calcic to alkalic (Frost et al., 2001). On the tectono-magmatic discrimination diagrams of Pearce et al. (1984) and Harris et al. (1986) the Terlemez and Baranadag quartz-monzonites show some complexity in the source regions as post-collisional granitoids, while the Hisarkaya porphyritic granite and the Çamsari quartz-syenite display syn-collisional and within-plate natures, respectively (Köksal et al., 2004; Köksal, 2005).

On primitive mantle-normalized multi-element plots (Fig. 2) all studied granitoids show enrichment in the large ion lithophile elements (LILE, e.g., Rb, Ba, Th, and K) and in light rare earth elements (LREE, e.g., La, and Ce) relative to the high field strength elements (HSFE; e.g., Nb, Zr, Sm, and Y) and heavy rare earth elements (HREE), and are characterized by negative anomalies of Ba, Nb, and Ti. The Hisarkaya porphyritic granite differs from the Terlemez and Baranadag quartz-

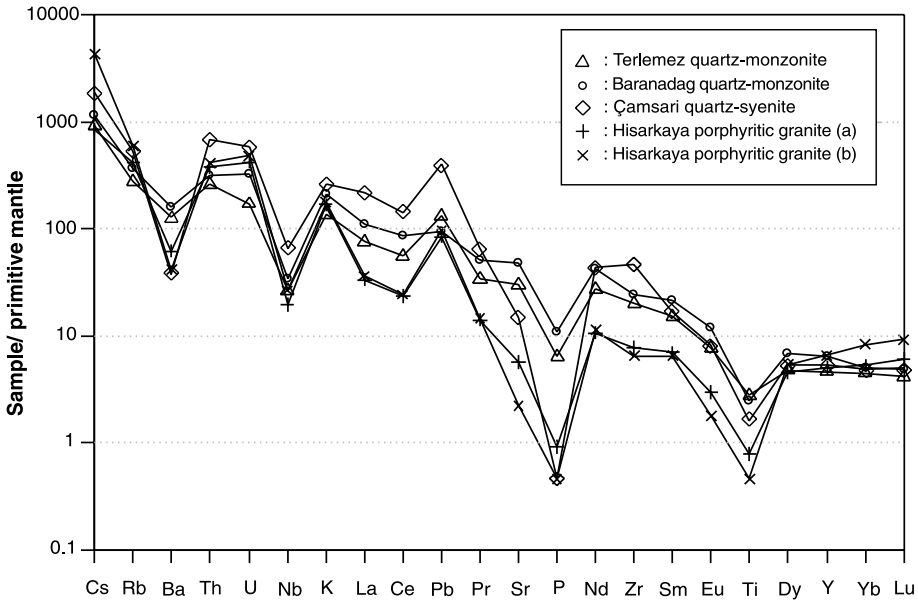

Fig. 2. Primitive mantle-normalized (after Sun and McDonough, 1989) trace-element patterns for the studied CAG. Data source: Table 1

monzonites by its higher SiO_2, Rb, Th, Yb, Lu, and its lower concentrations of Ca, Ba, Sr, P, Ti, Zr, La, Ce, Nd, Sm, and Eu (Fig. 2 and Table 1). The Çamsari quartz-syenite on the other hand shows the typical geochemical signature of A-type granitoids (Fig. 2 and Table 1), such as enrichment in Zr, Nb, Y and Ga, and REE (except Eu) and depletion of Ba and Sr (e.g., Whalen et al., 1987).

All chondrite-normalized REE patterns are steeply LREE-enriched and almost flat in HREE, but the Çamsari quartz syenite shows higher LREE and lower HREE contents [$(La/Yb)_N = 42$] than the I-type granitoids [$(La/Yb)_N = 16$ for Terlemez; 21 for Baranadag], while the Hisarkaya porphyritic granite has lower LREE values and higher HREE values [$(La/Yb)_N = 4–6$] than the others (Fig 2). The Terlemez and Baranadag quartz-monzonites and the Çamsari quartz-syenite have small negative Eu anomalies, $(Eu/Eu^*)_N = 0.64$, 0.75, and 0.60, respectively, whereas the Hisarkaya porphyritic granite have more pronounced negative Eu anomaly [$(Eu/Eu^*)_N = 0.27–0.52$)] (Table 1).

High initial $^{87}Sr/^{86}Sr$ isotope ratios (0.7078 to 0.7087) and noticeably negative $\varepsilon Nd_{(T)}$ data (-5.4 to -7.2) indicate significant involvement of crustal material within the petrogenesis of the studied granitoids (Köksal and Göncüoglu, in press).

Consequently, based on the petrological characteristics described above and interpretations of previous studies, the Terlemez and Baranadag quartz-monzonites were sampled to represent post-collisional I-type CAG, and the Çamsari quartz-syenite was sampled to represent post-collision or post-collisional extension related A-type CAG. The Hisarkaya porphyritic granite on the other hand shows typical features of syn- to post-collisional S- to I-type CAG (e.g., high SiO_2, Rb, Th, HREE, and low Ca, HFSE, and LREE) but some of its features (e.g., very low P_2O_5 values) infer similarities to aluminous A-type granitoids (e.g., Bonin, 2007). Therefore the Hisarkaya granitoid can be described as fractionated I-type granitoid with a notable crustal signature.

Analytical methods

The samples were crushed, ground and sieved to $< 500\,\mu m$, and the heavy mineral fraction including zircon was enriched with a Wilfley table, heavy liquid and magnetic (Frantz isodynamic magnetic separator) mineral separation. Zircon fractions were purified by handpicking from five granitoid samples (i.e., Terlemez, Baranadag, Hisarkaya-a, Hisarkaya-b, and Çamsari). After obtaining all available zircon crystals from the granitoid samples, only the unbroken and euhedral zircon crystals representing the zircon populations in these granitoids were separated for typological investigations. Between 128 and 387 crystals from each sample were selected for typologic investigation under a binocular microscope and at least 12 typical crystals were selected for scanning electron microscope (SEM) and CL studies. The selected grains were mounted on stubs such that they could be removed easily for further investigation. SEM and CL studies were carried out at the GeoForschungsZentrum Potsdam with a scanning electron microscope DSM 962/Zeiss equipped with a polychromatic Zeiss CL detector, using a 15 kV accelerating potential. Overviews and morphology images of the gold-palladium coated single zircons were taken with the back scattered electrons (BSE)-detector. The same grains were then polished down to half their thickness and carbon-coated for the CL-study.

Zircon classification was based on the zircon typology method of Pupin (1980). Each crystal was described considering its relative development of the crystal surfaces. The distributions of morphological types are shown on the typologic diagram for each sample. Typologic evolution trends of the samples were drawn based on the relative abundance of the types. We do not attempt to use zircon typology as a geo-thermometer, because this possible interpretation of the Pupin scheme is debatable according to the discussion given above (e.g., Vavra, 1990, 1993; Benisek and Finger, 1993).

Zircon typology

Overview of Pupin's approach

The zircon typology method proposed by Pupin (1980) basically expresses the arrangement of morphological types of zircon on the zircon typologic diagram based on the relative development of {100} and {110} prisms and {101} and {211} pyramids. Chemical composition of the melt affects the relative growth of zircon pyramids according to Pupin (1980). For example, the {211} pyramid dominate in zircon originating in a hyperaluminous or hypoalkaline medium, while the {101} pyramid is characteristic for hyperalkaline or hypoaluminous medium. Accordingly, the {301} pyramid is interpreted to be characteristic for zircon crystals formed in a potassium-rich alkaline medium (e.g., Pupin, 1980). Thus, Pupin (1980) suggested that the Al/alkaline ratio controls the A-index (A.I.) of a zircon population.

The typologic distribution has been determined on the basis of the examination of 100 to 150 unbroken zircon crystals whenever possible, and the coordinates in I.A. and I.T. (temperature index) space are computed (Pupin, 1980).

I.A. and I.T. are calculated by the following formulas:

$$\text{I.A.} = \sum_{\text{I.A.}=100}^{800} \text{I.A.} \times n_{\text{I.A.}} \qquad \text{I.T.} = \sum_{\text{I.T.}=100}^{800} \text{I.T.} \times n_{\text{I.A.}}$$

where $n_{\text{I.A.}}$ and $n_{\text{I.T.}}$ are the relative frequencies for each value of I.A. or I.T. ($\Sigma n_{\text{I.A.}} = \Sigma n_{\text{I.T.}} = 1$). The Typologic Evolution Trend (T.E.T.) is drawn through the mean point (I.A. and I.T.) with a slope $a = S_T/S_A$ which is the tangent of the angle between the T.E.T. axis and the A-index axis.

$$\text{Standard deviation of A-index} = S_A = \sqrt{(A - A_{\text{mean}})^2/n}$$

$$\text{Standard deviation of T-index} = S_T = \sqrt{(T - T_{\text{mean}})^2/n}$$

n = number of investigated crystals

Pupin (1980) proposed that the typologic study of zircon populations from granitic rocks can be used as a genetic classification, with three main divisions as (a) granitoids of crustal (or mainly crustal) origin, (b) hybrid (crustal and mantle origin) granitoids, and (c) granitoids of mantle (or mainly mantle) origin. On the typology diagram, granitoids of different origin show different zircon populations and distinct T.E.T.'s (Pupin, 1980).

Table 2. *Statistical zircon typology elements*[1] *of the studied Central Anatolian Granitoids*

Sample	I.A.	I.T.	S_A	S_T	A	$\alpha(^\circ)$	n
Terlemez	501	680	66.78	43.45	0.65	33	223
Baranadag	536	731	64.41	60.96	0.95	43	128
Hisarkaya-a	679	376	67.26	115.53	1.72	60	387
Hisarkaya-b	700	333	6.70	89.82	13.41	86	223
Çamsari	699	795	10.89	22.21	2.04	64	251

[1] I.A. and I.T. Mean points where T.E.T. (typlogical evolution trend) is drawn through, S_A Standard deviation of A-index, S_T Standard deviation of T-index, α Angle between the T.E.T. axis and the A-index axis, A S_T/S_A (slope of T.E.T., i.e., tangent α), n number of investigated crystals (Please see the text and Pupin, 1980 for detailed explanations)

Crustal granitoids, generally including leucogranites and aluminous monzogranites with no or little basic microgranular enclaves, are characterized by low A- and T-indexes (Pupin, 1980). The granitoids in the hybrid-group are mainly calc-alkaline or sub-alkaline monzogranites and granodiorites typically including basic microgranular enclaves in varying quantities and they show zircon populations having large ranges of A- (higher than those of crustal ones) and T- (from very high to low) indexes (Pupin, 1980). Alkaline granitoids are interpreted to be represented in the group of mantle or mainly mantle origin with zircon showing very high A- and T-index values (Pupin, 1980). It is plausible to classify *Pupin*'s crustal granitoids (Groups 1, 2, and 3) as S-type, hybrid granitoids (Groups 4 and 5) as I-type and mantle originated alkaline granitoids (Group 6) as A-type granitoid on the basis of petrological criteria (e.g., Finger et al., 1992; Schermaier et al., 1992).

Application of zircon typology method to the Central Anatolian granitoids

The zircon typology method (Pupin, 1980), based on the external morphology of zircon crystals was applied to some granitoids from Central Anatolia and statistical results are given in Table 2.

The Terlemez and Baranadag quartz-monzonites

Zircon crystals from the Terlemez and Baranadag quartz-monzonites range from colourless to pale yellow and yellow. Long prismatic crystals with extensive apatite inclusions are characteristic features for the zircon populations of these granitoids. The Terlemez quartz-monzonite shows mainly the zircon types S_{24} (e.g., Fig. 3a and b) and S_{25} and fewer grains of the $S_{13\text{-}18\text{-}19\text{-}20\text{-}23}$ types. Similarly, $S_{24\text{-}25}$ type zircons, as well as the J_5 type are predominant in the Baranadag quartz-monzonite, whereas $S_{15\text{-}18\text{-}19\text{-}20\text{-}23}$ and $J_{3,4}$ are less common types. Fig. 3c is an example for a S_{18} type zircon crystal while Fig. 3d shows an example of a S_{25} zircon type in the Baranadag quartz-monzonite.

Both granitoids show a relatively narrow range of zircon types with high T-index on the typology diagram (Fig. 4). T.E.T.s of Terlemez (Fig. 4a) and Baranadag (Fig. 4b) granitoids are similar and can be classified as stock 4c of Group-4 (after Pupin, 1980). According to Pupin (1980), zircons of Group-4 are

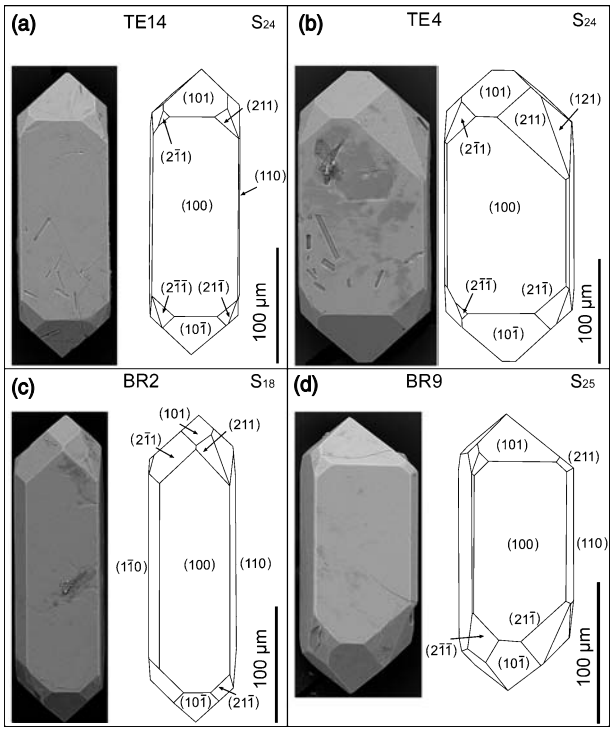

Fig. 3. SEM photographs and sketch models showing the crystal surfaces of the zircon crystals from the hybrid-type Terlemez and Baranadag granitoids: (**a**) TE14, (**b**) TE4, (**c**) BR2, (**d**) BR9

typical for granitoids that are hybrid calc-alkaline series granites that typically have inclusions of basic microgranular xenoliths in varying quantities and are sometimes associated with basic rocks (gabbro, quartz gabbro, diorite, and quartz diorite). Subgroup (stock) 4c of this group mainly comprises biotite ± amphibole ± pyroxene granodiorite, biotite ± amphibole ± pyroxene monzogranite, and biotite ± secondary muscovite alkaline granite (Pupin, 1980). This subgroup is also said to be characterized by presence of frequent microgranular basic xenoliths (Pupin, 1980). These features are consistent with the geological and petrographic characteristics of the Terlemez and Baranadag quartz-monzonites.

The Çamsari quartz-syenite

The zircon population of the Çamsari quartz-syenite ranges from dark brownish, yellow, pale yellow to rare colourless or white varieties. The major zircon type is a K-type (Fig. 5a), while other observed types are V_{25} (Fig. 5b) and T_5. These types are characterized by the existence of (301)-pyramid surfaces. The zircon crystals typically demonstrate preferential development of the {101} pyramid and notably the occurrence of the {301} pyramid. Zircon types from the Çamsari quartz-syenite are located along the right hand-side part of the typology diagram with very high A- and T-indexes (Fig. 6).

Radial cracks are visible on most of the zircon crystals from the Çamsari quartz-syenite (e.g., Fig. 5a). These cracks can be interpreted as the result of volume expansion due to metamictization (e.g., Murakami et al., 1991). Metamictization is the process of lattice destruction by radiation damage (e.g.,

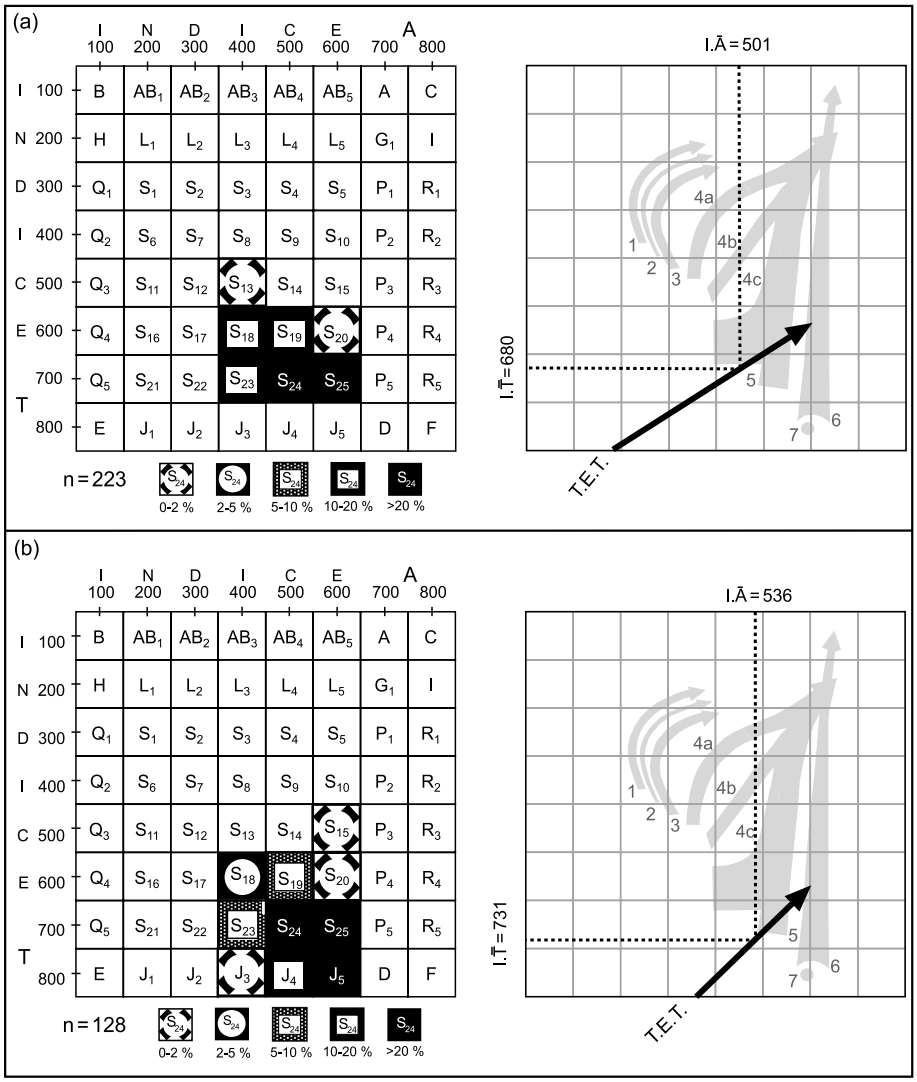

Fig. 4. Distribution of zircon crystals from the hybrid-type Terlemez and Baranadag granitoids on the typologic diagram of Pupin (1980) and the constructed Typologic Evolution Trends (T.E.T.) with the average values (I.A. and I.T.): (**a**) Terlemez granitoid, (**b**) Baranadag granitoid, ''n'' designates the number of crystals examined. Distribution of means for I.A. and I.T. and mean Typologic Evolution Trend (T.E.T.) of zircon populations from: Granites of crustal or mainly crustal origin [(*1*) aluminous leucogranites; (*2*) (sub) autochthonous monzogranites and granodiorites; (*3*) intrusive aluminous monzogranites and granodiorites], granites of crustal+mantle origin or hybrid granites [(*4a, b, c*) calc-alkaline series granites; (*5*) sub-alkaline series granites], granites of mantle or mainly mantle origin [(*6*) alkaline series granites; (*7*) tholeiitic series granites] (Pupin, 1980)

Williams, 1992), and it occurs at temperature conditions at which annealing of the lattice is slower than the damage accumulates, and therefore more severe in zircon with high U and Th concentrations. Raman spectra of Sri Lanka zircons reveal that increasing radiation damage results in irregular atomic positions, bond lengths and

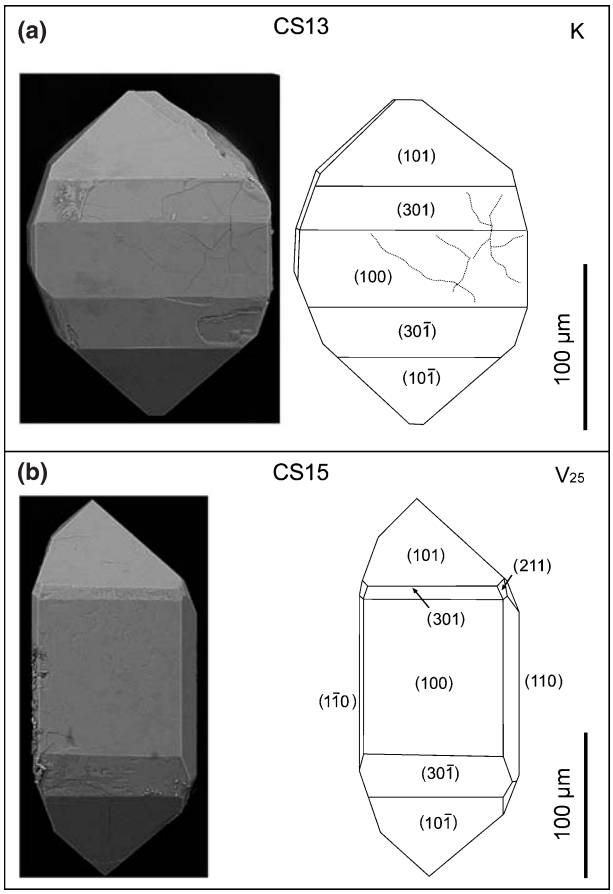

Fig. 5. SEM photographs and sketch models showing the crystal surfaces of zircon crystals from the Çamsari granitoid: (**a**) CS13, (**b**) CS15

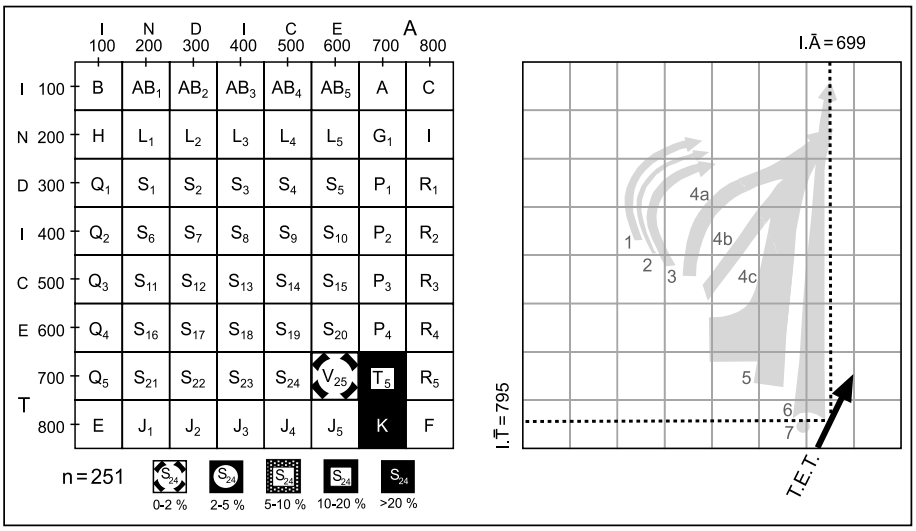

Fig. 6. Distribution of zircon crystals from the alkaline-type Çamsari granitoid on the typologic diagram of Pupin (1980) and corresponding T.E.T. ''n'' designates the number of crystals examined

bond angles in zircon, which tends to be amorphous at full metamictization (Nasdala et al., 2001). Heterogeneous distribution of U and Th in zircon may cause heterogeneous metamictization (Nasdala et al., 1998) leading to local stress and formation of micro-fissures and cracks due to heterogeneous expansion (Nasdala et al., 2001).

T.E.T. and crystal types of the A-type Çamsari quartz-syenite are similar to Group-6, which are alkaline series granitoids with mantle or mainly mantle origin according to Pupin (1980) (Fig. 6). Alkaline and hyperalkaline granitoids found in subvolcanic, anorogenic complexes are interpreted to be part of this group (Pupin, 1980). Iron-rich minerals (e.g., hedenbergite) are typical for these granitoids (Pupin, 1980), and this is consistent with their presence in the Çamsari quartz-syenite sample.

The Hisarkaya porphyritic granite

The Hisarkaya porphyritic granite is sampled from two different intrusive stocks i.e., samples Hisarkaya-a and Hisarkaya-b. The zircon population of the Hisarkaya porphyritic granite consists mainly of dark brownish, pale yellow and some colourless or white varieties with rare apatite and titanite inclusions. In general, the zircon types in the samples Hisarkaya-a and Hisarkaya-b are similar, but Hisarkaya-b contains only a subset of the types found in Hisarkaya-a and has different abundances. The most abundant zircon types are $P_{1\text{-}2\text{-}3}$ and G_1, while P_4 and $S_{4\text{-}5\text{-}7\text{-}9\text{-}10\text{-}11\text{-}12\text{-}13\text{-}14\text{-}15\text{-}19\text{-}20}$ are rarely present. G_2 and G_3 types are rare in Hisarkaya-a, but abundant in Hisarkaya-b. Asymmetrical evolution of the pyramid surfaces in the zircon crystals is common in these crystals. A P_4 type zircon crystal HKa17 with a large (100)-prism face in front is presented in Fig. 7a, while a typical S_4 type crystal HKa4 characterized by minor development of the (121)-pyramidal face is shown in Fig. 7b. The zircon population in the Hisarkaya porphyritic granite is characterized by a high A-index, indicative of a high Al/alkaline ratio, while the T.E.T. of Hisarkaya-b (HKb) is steeper than that of Hisarkaya-a (HKa) (Fig. 8). The case of the Hisarkaya porphyritic granite exemplifies that different outcrops from the same granitoid may show different zircon typologic characteristics to some extent.

The zircon population of the Hisarkaya porphyritic granite tends toward the G-type on the end of its evolution trend, and resembles Group-4 for Hisarkaya-a and

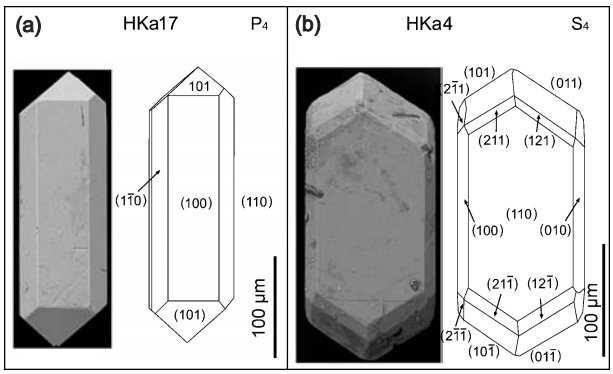

Fig. 7. SEM photographs and sketch models showing the crystal surfaces of zircon crystals from the crustal-type Hisarkaya granitoid: (**a**) HKa17, (**b**) HKa4

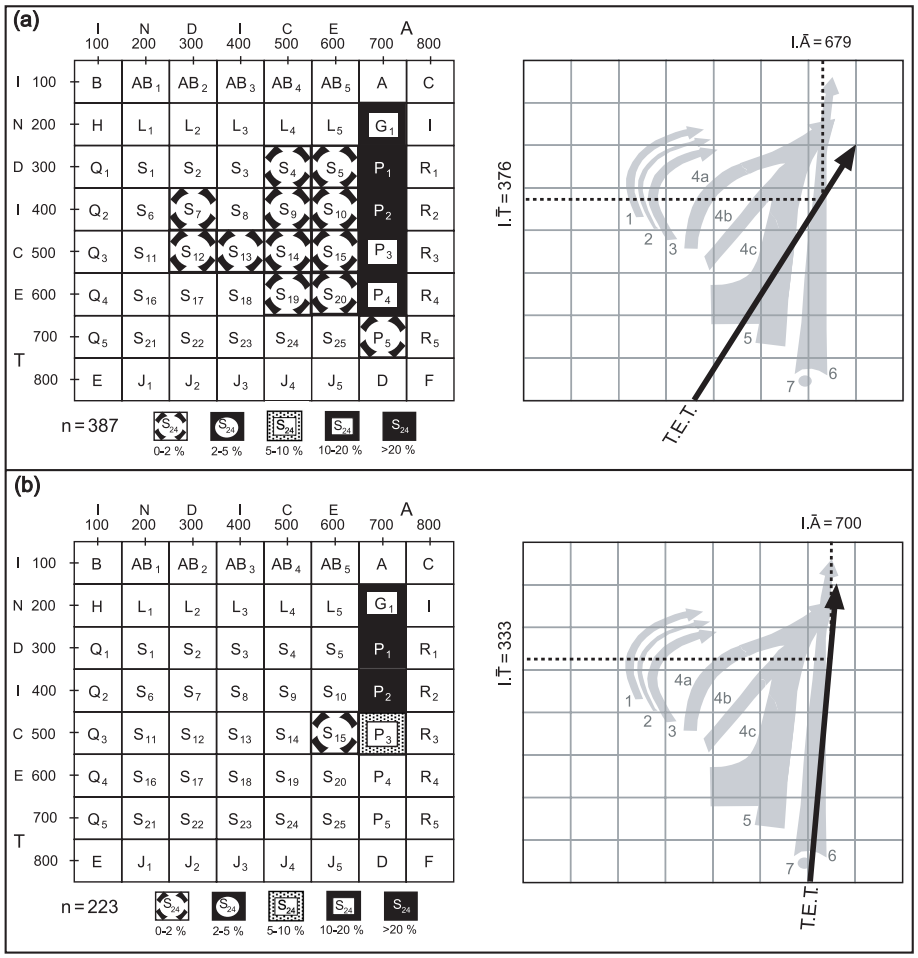

Fig. 8. Distribution of zircon crystals from two samples of the crustal-type Hisarkaya granitoid on the Pupin (1980) typologic diagram and corresponding T.E.T.s: (**a**) Hisarkaya-a, (**b**) Hisarkaya-b, ''n'' designates the number of crystals examined

Group-6 for Hisarkaya-b samples. Depending on the typologic evolution trends of samples Hisarkaya-a and Hisarkaya-b, the Hisarkaya porphyritic granite maybe described as either I- or A-type granitoid (Fig. 8). Partial overgrowths (observed under binocular microscope) are common in the Hisarkaya porphyritic granite, and are interpreted here as evidence for discontinuities in the growth history (e.g., Speer, 1982). Therefore it should be noted that changing external typologic features could be expected during the growth history of zircon in this granitoid.

Internal structures of zircon crystals

Sixteen zircon crystals from the Terlemez, 15 crystals from the Baranadag, 10 zircon crystals from the Hisarkaya-a, 6 crystals from the Hisarkaya-b and 18 crystals from the Çamsari granitoids were imaged by CL. Data obtained from the CL study along with detailed information on internal structures of most representative crystals are presented below.

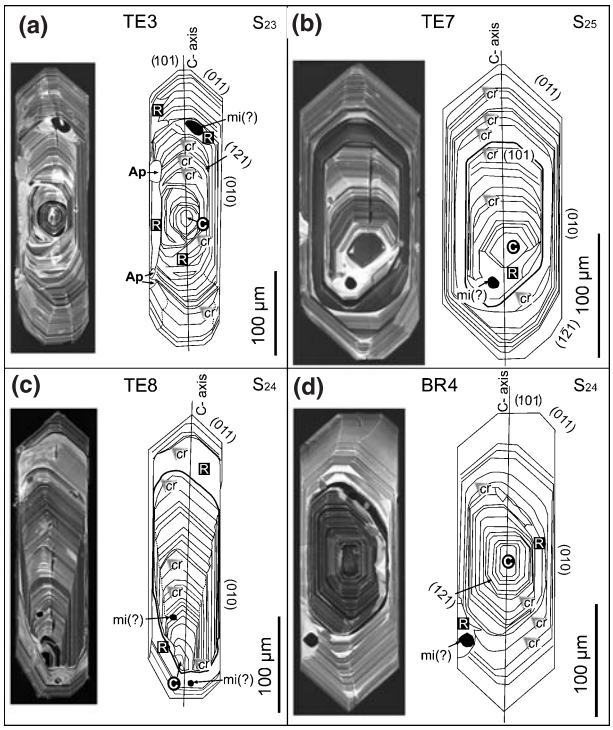

Fig. 9. CL photographs and sketches showing the internal structures of zircon crystals from the hybrid-type Terlemez and Baranadag granitoids: (**a**) TE3, (**b**) TE7, (**c**) TE8, (**d**) BR4. Abbreviations are; *C* core, *R* recrystallized domains or recrystallization patches, cr: corrosion (resorption or dissolution), *T* thickened trace element rich band, *M* metamictized domains, *mi*(?) possible melt inclusion, *Ap* apatite inclusion

The Terlemez and Baranadag quartz-monzonites

Zircon crystals from Terlemez and Baranadag quartz-monzonites are characterized by oscillatory zoning with intermittent dissolution surfaces (Fig. 9). Smoothly rounded dissolution surfaces (marked cr) represent corrosion or resorption events during evolution of a zircon crystal (e.g., Vavra, 1990, 1994). Recrystallization patches (loss of oscillatory zoning, often around inclusions, e.g., Pidgeon, 1992) and low-CL intensity rims are typical features in these samples. Apatite and melt inclusions are common in zircons from the Terlemez and Baranadag quartz-monzonites.

Internal structure of a S_{23}-type zircon crystal TE3 is shown in a section parallel to the (100) prism face (Fig. 9a). Zones with oscillatory zoning with intermittent resorption surfaces overgrow the core (marked C) and surrounding corroded layers. It can be seen that during growth periods immediately after corrosion stages, at conditions below Zr-supersaturation, (010)-prisms form with low growth rate, represented by wide-dark CL-bands conformable with the inner surface (cf. Vavra, 1994). The outer shell is characterized by flow structures and recrystallized patches (marked R). Irregular shaped dashed lines designate sector boundaries.

A S_{25}-type zircon crystal TE7 is sectioned parallel to the (100)-prism face (Fig. 9b), showing resorption and truncation of an oscillatory-zoned inner part. Truncations of the oscillatory zones are interpreted as chemical corrosion events (supposed surface at the time of a major corrosion event is shown by a bold line). The subsequent internal structures can be divided into two broad zones as; (i) a CL-dark inner zone, and (ii) a CL-bright zone that continues to the rim of crystal. The notable decrease of the growth rate of the (010)-prism is remarkable. Vavra (1994)

interpreted that the cooling rate of the crystallizing magma is the fundamental factor controlling the Zr-supersaturation and accordingly the relative growth rate of (010)-prisms. The repeated intervals of zircon growth with low (010)-prism growth rate, interrupted by crystal corrosion as seen in this sample, are thus consistent with low Zr-supersaturation (Vavra, 1994).

A S_{24}-type zircon crystal TE8 is sectioned parallel to the (100)-prism face (Fig. 9c). The crystal shows a complex history of development beginning with euhedral oscillatory zones, which overgrow the small core and surrounding resorption surface, in the direction of the c-axis. Intermittent corrosion stages result in low growth rate of the (010)-face. After this period of probable magmatic growth the elongate crystal was broken (indicated by the presence of only one half of the pre-corrosion-surface grain, similar to crystal TE7) and/or resorbed. Subsequent growth of a recrystallized band is followed by further corrosion at the upper end of the crystal. These recrystallization patterns are likely related with late stage interaction between zircon and fluids formed during cooling and crystallization of the granitoid, combined with secondary trace element migration and loss (e.g., Pidgeon et al., 1998). The outer part of the crystal is characterized by further oscillatory growth.

A S_{24}-type zircon crystal BR4 is sectioned parallel to the (100)-prism face (Fig. 9d). The crystal can be differentiated into two main parts, an internal CL-

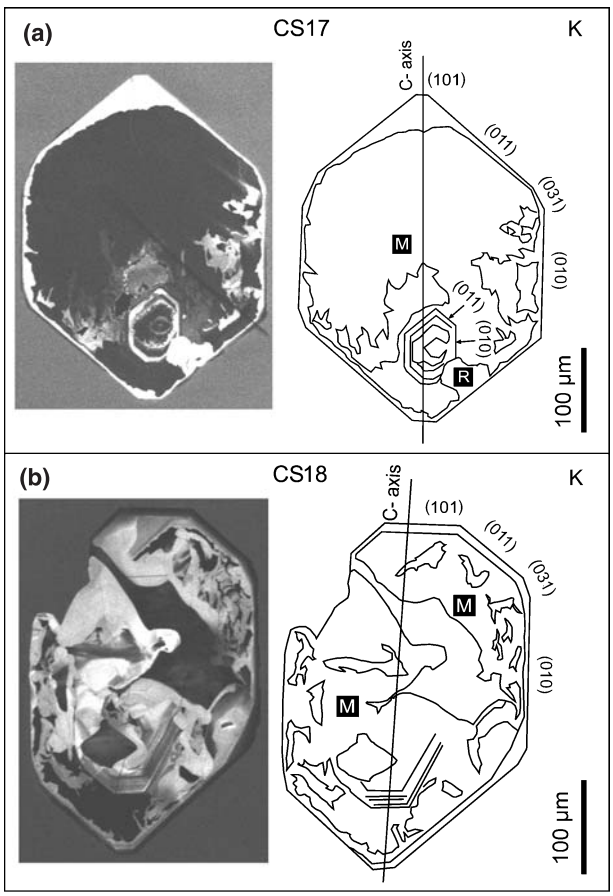

Fig. 10. CL photographs and sketches showing the internal structures of zircon crystals from the alkaline-type Çamsari granitoid: (**a**) CS17, (**b**) CS18. Abbreviations as in Fig. 9

dark and an outer CL-bright one. There are minor resorption zones within the internal part, but the foremost resorption stage is characterized by a wide CL-dark zone (outside the zone marked R) between the two main oscillatory zones.

The Çamsari quartz-syenite

Internal structures of zircon crystals from the Çamsari quartz-syenite show features characteristic for changing chemical conditions (Fig. 10).

The zircon crystal CS17 is sectioned parallel to the (100) prism face (Fig. 10a). A small core with (010) and (011)-faces are distinct from the main large crystal, which characterizes an alkaline environment. The crystal is characterized by a large, low-CL and extensively metamictized zone, also evident from radial cracks. Rapid growth of (010) favours the presence and increasing size of (031) (e.g., Vavra, 1994). These features are typical for most of the zircon crystals from the Çamsari quartz-syenite examined by CL. The outer shell of the crystal, defining the external morphology, is mostly very CL-bright (indicative of low trace element content and good crystallinity) with no discernible internal features, but is overlain by an extremely thin CL-dark rim.

The zircon crystal CS18 is also sectioned parallel to the (100)-prism face (Fig. 10b). Like the crystal CS17 it is metamict, even the oscillatory zoning in the internal part has been almost completely obliterated by metamictization.

The Hisarkaya porphyritic granite

Zircon from the Hisarkaya porphyritic granite is commonly characterized by CL structures revealing cores, interpreted to be inherited, because they are structurally discontinuous to the outer growth zones, show truncated zoning as well as blurred and convoluted zoning (this is interpreted as metamictization, evident from radial cracks in the surrounding growth zones, a feature more common in HKb) surrounded by relatively brightly luminescent zones, followed by low luminescent zones with (011)- and (110)-faces (Fig. 11). Zircon in samples Hisarkaya-a and Hisarkaya-b shows similar CL features, with slight differences, consistent with the similarity in the external morphological characteristics.

The zircon crystal HKa6 is of S_{15}-type and sectioned parallel to the (110)-prism face (Fig. 11a). The large CL-dark, inherited core (metamict, note radial fractures)

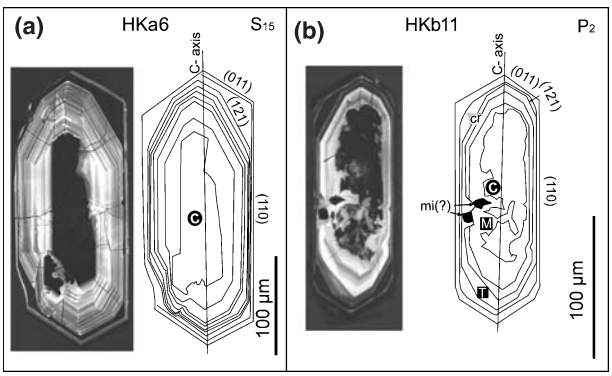

Fig. 11. CL photographs and sketches showing the internal structures of zircon crystals from the crustal-type Hisarkaya granitoid: (**a**) HKa6, (**b**) HKb11. Abbreviations as in Fig. 9

in this zircon is overgrown by oscillatory zoned material that results in a crystal outline dominated by (121)-pyramid faces. Rapid growth intervals of (011)-faces increased the size of the adjacent (121)-pyramids (e.g., Vavra, 1994). Increasing growth rate of (011)-faces is suggested to be associated with adsorption of cations like Na, K and Al, which change relative surface energies of the possible structures (Vavra, 1994). The (121)-pyramid dominated crystal outline has a sharp transition to the outer, CL-dark and morphologically distinct, zone. This sharp morphological and chemical discontinuity (drop in CL-intensity) at the latest stages of zircon crystallization is difficult to explain by changing cooling rate or Zr-supersaturation and chemical composition of the magma (Vavra, 1994). Increased concentration of impurity elements like U, Th, Y, P, and REEs however, can result in the drop in CL-intensity and may dramatically change the morphological evolution of zircon (Vavra, 1994) as observed here. The outer rim of the crystal is characterized by medium CL-intensity.

The zircon crystal HKb11 is sectioned parallel to the (110)-prism face (Fig. 11b). The core is metamict (note radial fractures in CL-bright zones) and corroded, and the overgrowing brightly luminescent zone is characterized by predominant (121)-pyramids and presence of melt inclusions. Distortion in the left part of internal zones is likely to be related to these melt inclusions. This central part is surrounded by a broad, trace element rich band, as in crystal HKa6. Asymmetric evolution and size of (121)-pyramid are probably controlled by the growth rate of adjacent (011)-faces. The outer rim of the crystal with P_2-type crystal morphology is formed by alternation of medium and dark-CL zones.

CL-images of the zircon crystals from the Hisarkaya porphyritic granite reveal interesting evolutionary histories. Zircon cores in this granitoid are dominated by {121}-pyramids and can be described as S_2, S_7, S_{12} or S_{13}-zircon types, which are characteristic for S-type granitoids. Thus internal zircon typologies provide contradictory data with respect to the information obtained from the external zircon morphologies. Additionally these metamict and inherited cores that were discontinuously overgrown by non-metamict zones may point out evidence for a low temperature, detrital history. The highly different core and rim ages detected by the LA-ICP-MS U-Pb dating (Köksal et al., unpublished data) also support this interpretation.

Discussion

External and internal zircon habits and structures have the potential to be linked to complex magma evolution histories from initial formation by source melting, through stages of movement through the crust, contamination and mixing with different magma batches, fractional crystallization and differentiation, with loss of cumulates and vapour, and final emplacement or extrusion (Corfu et al., 2003). Typological characteristics of zircon crystals may show changes closely correlated with compositional zoning of granitoids (Siebel et al., 2006), and these may change throughout the magmatic history within a single zircon crystal (e.g., Belousova et al., 2006). It is widely known that the growth zones in zircons of igneous rocks result from physical and chemical variations in the melt or solutions

from which the zircon crystallizes and a lack of re-equilibration (Speer, 1982). Details about their origin, however, have remained enigmatic.

The zircon structures from the different types of granitoids in Central Anatolia reveal noteworthy characteristics. When evaluated on the basis of the zircon typology method, there is no doubt to classify the I-type granitoid samples of Terlemez and Baranadag as hybrid calc-alkaline series granitoids, i.e., Group-4 of Pupin (1980). Considering zircon crystal distribution on the typology diagram and T.E.T.s, the Terlemez and Baranadag are akin to granitoids having sources hybridized from both crustal and mantle sources. Field, mineralogical and geochemical features of the Terlemez and Baranadag also reveal the hybrid-nature of these granitoids.

CL-images of the investigated zircon crystals from these I-type Terlemez and Baranadag quartz-monzonites reveal fine or medium-scale oscillatory zoning. Euhedral zircons are dominant, but some of the crystals have anhedral, relict cores with euhedral overgrowths. The most striking feature detected on the CL-images of the Terlemez and Baranadag zircons is the existence of multiple growth stages accompanied by intermittent corroded crystal outlines. This repeated corrosion of zircon in the magma chamber may be caused by the influx of hot magma, thus these resorption surfaces are likely to be related to magma mixing in the calc-alkaline magmas (e.g., Vavra, 1994). In some crystals significant change in zircon typology is also recognizable subsequent to corrosion zones (Fig. 9). These changes in zircon morphology within single grains may also be associated with distinct changes in trace element and Hf-isotope signatures, and reflect the magma mingling/mixing processes, hence changes in magma composition (e.g., Griffin et al., 2002; Belousova et al., 2006). These interpretations are in accordance with the hypothesis of mantle derived mafic melt injection in the evolution of monzonitic I-type CAG.

Corrosion surfaces within zircons from Terlemez and Baranadag quartz-monzonites are commonly surrounded by CL-dark zones immediately overgrowing these corrosion surfaces. Relationship between zircon chemistry and CL-intensity also is the subject of several studies (e.g., Hanchar and Miller, 1993; Poller et al., 2001). Zones of corrosion should reflect resorption of the inherited zircon until Zr-saturation was reached again. Moreover, trace elements like U, Th, Y, and REE, incompatible in many rock-forming silicate minerals because of their large ionic radii and high charge, generally become concentrated in the residual melts and are incorporated in zircon, because its crystal structure holds varying proportions of these elements (Belousova et al., 2002). Poller et al. (2001) stated that U and related radiation (and possibly Hf) may suppress the CL-intensity, whereas CL-intensity show no direct correlation with the REEs, Y, or Th contents. Some studies (e.g., Ohnenstetter et al., 1991; Rubatto and Gebauer, 2000) on the other hand, show negative correlation between Y and the CL-intensity. Rubatto and Gebauer (2000) instead suggested that trace element content controls the CL-intensity, and uranium behaviour should be systematically related with other trace elements. Some authors (e.g., Marfunin in Marshall, 1988; Hanchar and Miller, 1993) indicated that luminescence is possibly caused principally by Dy^{3+}. On the other hand, Kempe et al. (2000) demonstrated with CL-spectra that in most cases line groups related to the emission of REE^{+3} (dominantly Dy^{+3}) are superimposed on broad

bands of varying intensity, thus suggesting that CL-emission is a complex signal caused by different emission centers.

In spite of the debate about the source of CL-intensity, what is commonly accepted for non-metamict zircon is that the CL-bright zones generally show enrichment of REE^{+3} (especially Dy^{+3}), while CL-dark zones generally have high U, Th, and Y contents. Therefore, it is reasonable to state that the resorption zones within zircons from the hybrid-type granitoids in this study are accompanied by decrease in Zr and REE, and increase in U, Th, and Y. Accordingly, Rubatto and Gebauer (2000) suggested that the higher diffusion rates of U and other trace elements in hotter melts result in broad CL-dark zones around resorbed zircons. Dissolution and re-growth of zircon can be caused by transient heating of the resident felsic magma by a mafic melt contribution which is an effective way of raising the temperature in felsic magma for short periods of time, even with modest amounts of basaltic input (e.g., Sparks and Marshall, 1986; Miller and Wooden, 2004). Therefore we suggest that the intermittent corrosion surfaces and subsequent CL-dark zones detected in Central Anatolian hybrid-type granitic zircons are related to magma mingling/mixing events, similar to interpretations of Belousova et al. (2006) for Australian granitoids.

In most of the zircon crystals there is one major and some additional minor zones of corrosion. The major corrosion zone may signify a main episode of mantle-derived mafic melt contribution to a felsic magma chamber or represent original melting of the crustal protolith material. Furthermore, narrow corrosion zones may be subsequent short periods of magma mingling, or cyclic dissolution and re-growth events during a long period of mafic melt injection. Hoskin and Schaltegger (2003) also indicated that zircon crystals with multiple corrosion surfaces record compositional data for the melt prior to and after dissolution and record changes possibly related to magma mixing and are therefore important witnesses to the magma evolution history. Alternatively, multiple dissolution and growth could be caused by movement of zircon within the different parts of the magma chamber having distinct thermal and chemical conditions. As indicated by Pidgeon and Compston (1992), magma may be inhomogeneous over an unspecified scale, and zircons can experience different crystallization histories in different parts of the magma before being finally brought together in the volume of granitoid represented by the present samples. Forced convection through mafic melt injection is one of the factors resulting in transportation of zircon crystals in a magma chamber (e.g., Snyder and Tait, 1996; Couch et al., 2001; Miller and Wooden, 2004). Detailed discussion of time-space relationships of magmatic events recorded in zircon crystals might be possible with complementary data from in-situ U-Pb dating of these zircons.

A-type granitoid sample Çamsari contains morphologically distinct zircon crystals with high A-index indicating alkali-rich magmas. A high cooling rate of the alkaline Çamsari quartz-syenite is deduced from high and constant growth rates of (010)- and adjacent (031)-pyramids in CL-images, based on the interpretation of Vavra (1994) (Fig. 10). Moreover, (110) faces are absent or rarely present, which is a characteristic feature in alkaline granitoids with an anhydrous mineral paragenesis (Vavra, 1994). Bonin et al. (1998) mentioned the presence of analogous zircon habits in post-orogenic granitoids. Post-orogenic granitoids evolve in the last mag-

matic episodes in an orogenic belt that becomes cratonic by cooling and thickening of lithosphere (Bonin et al., 1998). In a similar manner, the Çamsari quartz-syenite is interpreted as a post-collisional A-type granitoid marking the final stages of the collisional period in Central Anatolia (Köksal et al., 2004). Extensive metamictization is a characteristic feature for zircon crystals from the Çamsari quartz-syenite. Metamict micro-areas commonly contain higher concentrations of U, Th, Y, Ca, and Fe, with respect to neighbouring areas (Nasdala et al., 1996). Similarly, Kempe et al. (2000) have shown that metamictization results in the formation of low-CL zones enriched in trace elements (e.g., U, Th, Y, Yb, and P) and occasionally Fe and Ca.

While the morphological description of zircon crystals of I- and A-type granitoids in this study confirms the geological and geochemical features, it is not the case for zircons from the Hisarkaya porphyritic granite. Based on the zircon typology method, the Hisarkaya porphyritic granite reveals characteristics of I- to A-type granitoids. CL-images of the internal structures reveal additional information not observable from the external morphology (Fig. 11), namely the predominance of (121)-pyramids in the earlier stages of growth, typical for crystals from granitoids with dominantly S-type characteristics (e.g., Pupin, 1980; Schermaier et al., 1992). However, the (121)-pyramids disappear at the CL-dark rims, the crystal habit changes significantly and morphology turns to what is common in hybrid-type granitoids. The reason may be a rapid change in chemical conditions at the latest stages of crystallization. However, Vavra (1994) stated that this kind of sharp morphological and chemical discontinuity (decrease in CL-brightness) during the late stages of zircon crystallization is difficult to explain either by changing cooling rate, Zr-supersaturation or chemical composition of the magma. Alternatively, Vavra (1994) suggested that the formation of large growth increments (from elements with smaller ionic radii) in the liquid, before they assembled on the crystal, was likely to be the cause of these features (CL-dark, preferred growth of (010)-faces). The formation of growth units, including some impurity elements like U, Th, Y, P, and REE, starts when the magma attains sufficiently low temperatures and high concentration of essential elements (Vavra, 1994). Incidentally, partial overgrowths on the zircon crystals of Hisarkaya granitoid detected microscopically and inherited cores observable by CL imply discontinuities in zircon growth, typical phenomena for S-type granitoids (e.g., Speer, 1982). Therefore it is reasonable to interpret the cores of zircons of the Hisarkaya porphyritic granite to be formed in environments chemically distinct magmatic from those giving shape to the external zircon morphologies. Consequently, we suggest defining the Hisarkaya porphyritic granite as a crustally derived granitoid with a significant component of inherited zircon. Accordingly, Kemp et al. (2007) have demonstrated that a typical I-type granitoid can be formed from reworking of sedimentary materials by mantle-like magmas.

In summary, the observed zircon typologies are consistent with the geological and geochemical data for the studied I- and A-type granitoids. However, as has been inferred before (e.g., Vavra, 1993; Belousova et al., 2006) the typology method reveals information only depending on the final zircon morphologies of the granitoids, but may not represent their whole evolution histories, as demonstrated here with the Hisarkaya samples. Information gathered from typology studies is not

satisfactory by itself to evaluate zircon formation histories, and has to be complemented by the study of internal structures of crystals.

Conclusions

Investigation of the morphology and internal structures of zircons from the Central Anatolian Granitoids reveals that the I-type Terlemez and Baranadag quartz-monzonites contain zircon types and T.E.T.s typical for calc-alkaline series hybrid-granitoids, whilst the A-type Çamsari quartz-syenite has characteristic zircon types and the T.E.T. of alkaline granitoids (e.g., Pupin, 1980). This is completely in accordance with the field, mineralogical and geochemical characteristics. Zircons from the I-type Terlemez and Baranadag quartz-monzonites were subjected to intense corrosion at certain times of magmatic evolution, distinguishable on CL-images by obvious dissolution surfaces around cores and/or surrounding zones. These corrosion zones encompass low Zr and REE (especially Dy), and high U, Th, and Y contents. The resorption surfaces followed by new zircon growth zones are interpreted as evidence for magma mingling/mixing processes within the studied I-type-granitoids from Central Anatolia.

However, evaluation of the internal structures of zircon crystals from the Hisarkaya porphyritic granite reveals data antithetic to the external morphology of zircon populations. CL-images show abrupt morphological changes from the internal to the outer parts of the crystals that are interpreted to be related to combination of zirconium with particular trace elements in the magma to form ''growth units'' before deposited onto existing zircon crystal surfaces (e.g., Vavra, 1994). Thus for the Hisarkaya porphyritic granite it is concluded that the chemistry of the medium at the latest growth stages shaped the external morphologies of the crystals and conceals the typological characteristics of internal surfaces of the zircons that would be typical for S-type granitoids.

As a result, we suggest that zircon typological studies as proposed by Pupin (1980) can help to understanding the evolution histories of some granitoids, as in the case of Central Anatolian Granitoids, especially when they are combined with the CL-imaging of internal structures. These internal structures are crucial for an understanding of the sequence and history of crystallization of the magmas, whereas external morphology may be shaped by the last gasps of magma evolution and as a thin veneer cover the major crystallization phases.

Acknowledgements

S. Köksal gratefully acknowledges access to laboratory facilities at the GFZ-Potsdam. We acknowledge the Scientific and Technical Research Council of Turkey (TUBITAK; project codes YDABÇAG-101Y051 and YDABÇAG-106Y066) for supporting the field study and geochemical analyses. The authors wish to express their thanks to technical staff from the Geoscience Department of Potsdam University and the GFZ-Potsdam, especially U. Glenz for her spectacular work on SE- and CL-imaging. The authors would like to thank F. Finger and U. Klötzli who provided detailed and useful reviews of the manuscript and R. Abart for editorial handling.

References

Akiman O, Erler A, Göncüoglu MC, Güleç N, Geven A, Türeli K, Kadioglu YK (1993) Geochemical characteristics of granitoids along the western margin of the Central Anatolian Crystalline Complex and their tectonic implications. Geol J 28: 371–382

Aydin NS, Göncüoglu MC, Erler A (1998) Latest Cretaceous magmatism in the Central Anatolian Crystalline Complex: review of field, petrographic and geochemical features. Turk J Earth Sci 7: 259–268

Aydin NS, Önen P (1999) Field, petrographic and geochemical features of the Baranadag quartz monzonite of the Central Anatolian Granitoids, Turkey. Turk J Earth Sci 8: 113–123

Barbarin B (1990) Granitoids: mineral petrogenetic classifications in relation to origin and tectonic setting. Geol J 25: 227–238

Belousova EA, Griffin WL, O'Reilly SY, Fisher NI (2002) Igneous zircon: trace element composition as an indicator of source rock type. Contrib Mineral Petr 143: 602–622

Belousova EA, Griffin WL, O'Reilly SY (2006) Zircon crystal morphology, trace element signatures and Hf isotope composition as a tool for petrogenetic modelling: examples from eastern Australian granitoids. J Petrol 47: 329–353

Benisek A, Finger F (1993) Factors controlling the development of prism faces in granite zircons: a microprobe study. Contrib Mineral Petr 114: 441–445

Bonin B, Azzouni-Sekkal A, Bussy F, Ferrag S (1998) Alkali-calcic and alkaline post-orogenic (PO) granite magmatism: petrological constraints and geodynamic settings. Lithos 45: 45–70

Bonin B (2007) A-type granites and related rocks: evolution of a concept, problems and prospects. Lithos, special issue on A-type granites and related rocks through time. doi: 10.1016/j.lithos.2006.12.007

Boztug D (2000) S-I-A-type intrusive associations: geodynamic of significance of synchronism between metamorphism and magmatism in Central Anatolia, Turkey. In: Bozkurt E, Winchester JA, Piper JDA (eds) Tectonics and magmatism in Turkey and the surrounding area. Geol Soc London Spec Publ London 173: 441–458

Chappell BW, White AJR (1974) Two contrasting granite types. Pacific Geology 8: 173–174

Chappell BW, White AJR, Wyborne D (1987) The importance of residual source material (restite) in granite petrogenesis. J Petrol 28: 1111–1138

Collins WJ, Beams SD, White AJR, Chappell BW (1982) Nature and origin of A-type granites with particular reference to southeastern Australia. Contrib Mineral Petr 80: 189–200

Corfu F, Hanchar JM, Hoskin PWO, Kinny P (2003) Atlas of zircon textures. In: Hanchar JM, Hoskin PWO (eds) Zircon. Reviews in mineralogy and geochemistry, Vol 53, pp 469–500

Couch S, Sparks RSJ, Carroll MR (2001) Mineral disequilibrium in lavas explained by convective self-mixing in open magma chambers. Nature 411: 1037–1039

Didier J, Barbarin B (1991) Enclaves and granite petrology. Elsevier, Amsterdam, 625 pp

Düzgören-Aydin NS, Malpas J, Göncüoglu MC, Erler A (2001) A review of the nature of magmatism in Central Anatolia during the Mesozoic post-collisional period. Int Geol Rev 43: 695–710

Erler A, Göncüoglu MC (1996) Geologic and tectonic setting of the Yozgat batholith, northern Central Anatolian Crystalline Complex, Turkey. Int Geol Rev 38: 714–726

Finger F, Haunschmid B, Schermaier A, Von Quadt A (1992) Is zircon morphology indicative of a mantle or crustal origin of a granite? Comparison of Pupin indices with Sr and Nd isotope data of 26 Austrian granites. Mitt Österr Mineral Ges 137: 135–137

Frost BR, Barnes CG, Collins WJ, Arculus RJ, Ellis DJ, Frost CD (2001) A geochemical classification for granitic rocks. J Petrol 42: 2033–2048

Göncüoglu MC, Türeli TK (1994) Alpine collision-type granitoids in the western Central Anatolian Crystalline Complex. J Kocaeli Univ 1: 39–46

Göncüoglu MC, Erler A, Toprak V, Olgun E, Yaliniz K, Kusçu I, Köksal S, Dirik K (1993) Geology of the central part of the Central Anatolian Massif: part III geological evolution of the Tertiary Basin of the Central Kizilirmak: Unpubl. Report No: 3313, Turkish Petroleum Company (in Turkish)

Göncüoglu MC, Köksal S, Floyd PA (1997) Post-collisional A-Type magmatism in the Central Anatolian Crystalline Complex: petrology of the Idis Dagi intrusives (Avanos, Turkey). Turk J Earth Sci 6: 65–76

Göncüoglu MC, Toprak GMV, Kusçu I, Erler A, Olgun E (1991) Geology of the western part of the Central Anatolian Massif: part I southern part: Unpubl. Report No: 2909, Turkish Petroleum Company (in Turkish)

Görür N, Oktay FY, Seymen I, Sengör AMC (1984) Paleotectonic evolution of Tuzgölü basin complex, central Turkey: In: Dixon JE, Robertson AHF (eds) The geological evolution of the Eastern Mediterranean. Geol Soc London Spec Publ. London, Vol 17, pp 81–96

Görür N, Tüysüz O, Sengör AMC (1998) Tectonic evolution of the Central Anatolian Basins. Int Geol Rev 40: 831–850

Griffin WL, Wang X, Jackson SE, Pearson NJ, O'Reilly SY, Xu X, Zhou X (2002) Zircon chemistry and magma genesis, SE China: in situ analysis of Hf isotopes, Pingtan and Tonglu igneous complexes. Lithos 61: 237–282

Güleç N, Kadioglu YK (1998) Relative involvement of mantle and crustal components in the Agaçören Granitoid (Central Anatolia-Turkey): estimates from trace element and Sr-isotope data. Chem Erde 58: 23–37

Hanchar JM, Miller CF (1993) Zircon zonation patterns as revealed by cathodoluminescence and back-scattered electron images: implications for interpretation of complex crustal histories. Chem Geol 110: 1–13

Hanchar JM, Rudnick RL (1995) Revealing hidden structures: the application of cathodoluminescence and back-scattered electron imaging to dating zircons from lower crustal xenoliths. Lithos 6: 289–303

Harris NBW, Pearce JA, Tindle AG (1986) Geochemical characteristics of collision-zone magmatism: In: Coward MP, Ries AC (eds) Collision tectonics. Geol Soc Spec Publ London, Vol 19, pp 67–81

Hoskin PWO, Schaltegger U (2003) The composition of zircon and igneous and metamorphic petrogenesis. In: Hanchar JM, Hoskin PWO (eds) Zircon. Reviews in mineralogy and geochemistry, Vol 53, pp 27–62

Ilbeyli N (2005) Mineralogical-geohemical constraints on intrusives in Central Anatolia, Turkey: tectono-magmatic evolution and characteristics of mantle source. Geol Mag 142: 187–207

Ilbeyli N, Pearce JA (2005) Petrogenesis of igneous enclaves in plutonic rocks of the Central Anatolian Crystalline Complex, Turkey. Int Geol Rev 47: 1011–1034

Ilbeyli N, Pearce JA, Thirlwall MF, Mitchell JG (2004) Petrogenesis of collision-related plutonics in Central Anatolia, Turkey. Lithos 72: 163–182

Irvine TN, Baragar WRA (1971) A guide to the geochemical classification of the common volcanic rocks. Canadian J Earth Sci 8: 523–548

Kadioglu YK, Güleç N (1999) Types and genesis of the enclaves in Central Anatolian Granitoids. Geol J 34: 243–256

Kadioglu YK, Dilek Y, Güleç N, Foland KA (2003) Tectonomagmatic evolution of bimodal plutons in the Central Anatolian Crystalline Complex, Turkey. Geol J 111: 671–690

Kemp AIS, Hawkesworth CJ, Foster GL, Paterson BA, Woodhead JD, Hergt JM, Gray CM, Whitehouse MJ (2007) Magmatic and crustal differentiation history of granitic rocks from Hf-O isotopes in zircon. Science 315: 980–983

Kempe U, Gruner T, Nasdala L, Wolf D (2000) Relevance of cathodoluminescence for the interpretation of U-Pb zircon ages, with an example of an application to a study of zircons from the Saxonian Granulite Complex, Germany. In: Pagel M, Barbin V, Blanc P, Ohnenstetter D (eds) Cathodoluminescence in geosciences. Springer-Verlag, Berlin, Heidelberg, pp 415–455

Köksal S (2005) Zircon typology and chemistry of the granitoids from Central Anatolia, Turkey. M.E.T.U., Unpubl Ph.D. Thesis, 314 pp

Köksal S, Romer RL, Göncüoglu MC, Toksoy-Köksal F (2004) Timing of post-collisional H-type to A-type granitic magmatism: U-Pb titanite ages from Alpine Central Anatolian Granitoids (Turkey). Int J Earth Sci 93: 974–989

Köksal S, Göncüoglu MC (in press) Sr and Nd isotopic characteristics of some S-, I- and A-type granitoids from Central Anatolia. Turk J Earth Sci

Köksal S, Göncüoglu MC, Floyd PA (2001) Extrusive members of postcollisional A-Type magmatism in Central Anatolia: Karahidir volcanics, Idisdagi-Avanos area, Turkey. Int Geol Rev 43: 683–694

Loiselle MC, Wones DS (1979) Characteristics and origin of anorogenic granites. In: Geol Soc America, Vol 11. Abs w Programs 468

Maniar PD, Piccoli PM (1989) Tectonic discrimination of granitoids. Geol Soc Am Bull 101: 635–643

Marshall DJ (1988) Cathodoluminescence of geological materials, Unwin Hyman, Boston, 146 pp

McDonough WF, Sun S-S (1995) The composition of the earth. Chem Geol 120: 223–254

Miller JS, Wooden JL (2004) Residence, resorption and recycling of zircons in Devils Kitchen Rhyolite, Coso volcanic field, California. J Petrol 45: 2155–2170

Murakami T, Chakoumakos BC, Ewing RC, Lumpkin GR, Weber WJ (1991) Alpha-decay event damage in zircon. Am Mineral 76: 1510–1532

Nasdala L, Beran A, Libowitzky E, Wolf D (2001) The incorporation of hydroxyl groups and molecular water in natural zircon ($ZrSiO_4$). Am J Sci 301: 831–857

Nasdala L, Pidgeon RT, Wolf D (1996) Heterogeneous metamictization of zircon on a microscale. Geochim Cosmochim Acta 60: 1091–1097

Nasdala L, Pidgeon RT, Wolf D, Irmer G (1998) Metamictization and U-Pb isotopic discordance in single zircons: a combined Raman microprobe and SHRIMP ion probe study. Mineral Petrol 62: 1–27

Ohnenstetter D, Cesbron F, Remond G, Caruba R, Claude J-M (1991) Emissions de cathodoluminescence de deux populations de zircons naturels: tentative d'interpretation. Comptes Rendues de l'Academie des Sciences, Serie II 313: 641–647

Otlu N, Boztug D (1998) The coexistence of the silica oversaturated (ALKOS) and undersaturated (ALKUS) rocks in the Kortundag and Baranadag plutons from the Central Anatolian alkaline plutonism, E Kaman/NW Kirsehir, Turkey. Turk J Earth Sci 7: 241–257

Pearce JA, Harris NBW, Tindle AGW (1984) Trace element discrimination diagrams for the tectonic interpretation of granitic rocks. J Petrol 25: 956–983

Pidgeon RT (1992) Recrystallization of oscillatory zoned zircon: some geochronological and petrological implications. Contrib Mineral Petr 110: 463–472

Pidgeon RT, Compston W (1992) Zircon Th-U-Pb systems as indicators of source rocks and magmatic processes: a SHRIMP study of four granites from the Scottish Highlands. Trans R Soc Edinburgh Earth Sci 83: 473–483

Pidgeon RT, Nemchin AA, Hitchen GJ (1998) Internal structures of zircons from Archean granites from the Darling Range batholith: implications for zircon stability and the interpretation of zircon U-Pb ages. Contrib Mineral Petr 132: 288–299

Poller U, Huth J, Hoppe P, Williams IS (2001) REE, U, Th, and Hf distribution in zircon from western Carpathian Variscan granitoids: a combined cathodoluminescence and ion microprobe study. Am J Sci 301: 358–376

Pupin JP (1980) Zircon and granite petrology. Contrib Mineral Petr 73: 207–220

Rubatto D, Gebauer D (2000) Use of cathodoluminescence for U-Pb zircon dating by ion microprobe: some examples from the western Alps. In: Pagel M, Barbin V, Blanc P, Ohnenstetter D (eds) Cathodoluminescence in geosciences. Springer-Verlag, Berlin, Heidelberg, pp 373–400

Schermaier A, Haunschmid B, Schubert G, Frasl G, Finger F (1992) Diskriminierung von S-typ und I-typ graniten auf der basis zirkontypologischer untersuchungen. Frankfurter Geowiss Arb Serie A Geologie-Paläontologie 11: 149–153

Siebel W, Thiel, M, Chen F (2006) Zircon geochronology and compositional record of late- to post-kinematic granitoids associated with the Bavarian Pfahl zone (Bavarian Forest). Mineral Petrol 86: 45–62

Snyder D, Tait S (1996) Magma mixing by convective entrainment. Nature 379: 529–531

Sparks RSJ, Marshall LA (1986) Thermal and mechanical constraints on mixing between mafic and silicic magmas. J Volcan Geothermal Res 29: 99–129

Speer JA (1982) Zircon. In: Ribbe PH (ed) Orthosilicates, 2nd edn, Reviews in mineralogy and geochemistry, Vol 5, pp 67–112

Sengör AMC, Yilmaz Y (1981) Tethyan evolution of Turkey: a plate tectonic approach. Tectonophysics 75: 181–241

Sun S-S, McDonough WF (1989) Chemical and isotopic systematics of oceanic basalts: implications for mantle composition and processes. In: Saunders AD, Norry MJ (eds) Magmatism in the Ocean Basins. Geol Soc London Spec Publ London, Vol 42, pp 313–345

Tatar S, Boztug D (2005) The syn-collisional Danaciobasi biotite leucogranite derived from the crustal thickening in Central Anatolia (Kirikkale), Turkey. Geol J 40: 571–591

Toksoy-Köksal F, Göncüoglu MC, Yaliniz MK (2001) Petrology of the Kurancali phlogopite metagabbro: an island arc-type ophiolitic sliver in the Central Anatolian Crystalline Complex. Int Geol Rev 43: 624–639

Vavra G (1990) On the kinematics of zircon growth and its petrogenetic significance: a cathodoluminescence study. Contrib Mineral Petr 106: 90–99

Vavra G (1993) A guide to quantitative morphology of accessory zircon. Chem Geol 110: 15–28

Vavra G (1994) Systematics of internal zircon morphology in major Variscan granitoid types. Contrib Mineral Petr 117: 331–344

Wang X, Griffin WL, O'Reilly SY, Zhou XM, Xu XS, Jackson SE, Pearson NJ (2002) Morphology and geochemistry of zircons from late Mesozoic igneous complexes in coastal SE China: implications for petrogenesis. Min Mag 66: 235–251

Whalen JB, Currie KL, Chappell BW (1987) A-type granites: geochemical characteristics, discrimination and petrogenesis. Contrib Mineral Petr 95: 407–418

Williams IS (1992) Some observations on the use of zircon U-Pb geochemistry in the study of granitic rocks, Trans. R. Soc. Edinburgh Earth Sci 83: 447–458

Yaliniz MK, Aydin NS, Göncüoglu MC, Parlak O (1999) Terlemez quartz monzonite of Central Anatolia (Aksaray-Sarikaraman): age, petrogenesis and geotectonic implications for ophiolite emplacement. Geol J 34: 233–242